

Feasibility Analysis of MERIS as a Tool for Monitoring Lake Guiers (Senegal) Water Quality

Seybatou Diop¹, Souléye Wade¹, Moshood N. Tijani²

¹Institute of Earth Sciences, Faculty of Sciences and Techniques, Cheikh Anta Diop University of Dakar, Dakar, Senegal

²Department of Geology, University of Ibadan, Ibadan, Nigeria

Email: seybdioop@yahoo.fr, wadesouleye@yahoo.fr, tmoshood@yahoo.com

Received 7 December 2015; accepted 23 January 2016; published 26 January 2016

Copyright © 2016 by authors and Scientific Research Publishing Inc.

This work is licensed under the Creative Commons Attribution International License (CC BY).

<http://creativecommons.org/licenses/by/4.0/>



Open Access

Abstract

ENVISAT/MERIS scenes of Lake Guiers covering the period 2003-2010 were processed for concentration retrieval of chlorophyll a (CHLa), suspended particulate matter (SPM) and colored fraction of dissolved organic matter (CDOM), *i.e.* the three main parameters relevant to the water quality management of the lake. Estimates in the range of 30 - 117 $\mu\text{g CHLa L}^{-1}$ (average 62.13 $\mu\text{g}\cdot\text{L}^{-1}$), 0.10 - 29.0 mg SPM L^{-1} (average 22.01 $\text{mg}\cdot\text{L}^{-1}$), and 1.10 - 1.90 CDOM m^{-1} (average 1.33 m^{-1}) were recorded, suggesting the possibility of occasional poor quality waters in some compartments of the lake. The values calculated as part of this study are consistent with literature data. On the basis of these estimates, interpretations were made as to the feasibility of applying MERIS data for synoptic environmental monitoring purposes. The data were subjected to statistical analysis, including regression analysis and significance tests. Estimates of CHLa and CDOM revealed some level of correlation, which suggests that phytoplankton biomass degradation may account for nearly 47% of the dissolved optical compounds CDOM. Notable areas of high CHLa and CDOM concentrations are found in the southern inshore zone, an environment with less water agitation. In contrast, SPM concentrations tend to increase in environments of very shallow water marked by high water turbulence and bottom mobility. However, it was not possible to fully assess the model performance and detection accuracy of the results due to lack of ground truths. Nonetheless, the results show concentrations that compared well with the *in-situ* data from earlier studies and data reported elsewhere from other lacustrine systems. Therefore, it can be inferred from this study that MERIS data present a useful low-cost (*i.e.* cost effective and readily available) approach for environmental monitoring of Lake Guiers waters with excellent spatial coverage. In addition, the study highlighted the minimal effect of the so-called “bottom effect” on model predictions, despite the small depth of the lake.

Keywords

Lake Guiers, MERIS, Environmental Monitoring, Water Quality, Chlorophyll a, Suspended Particulate Matter, Colored Dissolved Organic Matter

1. Introduction

Considerable interest has been focused in recent years on the role of satellite remote sensing data for surface water mapping and their application in lake-water quality monitoring ([1]-[3]). Basically, the procedure relies on analyzing the optical characteristics of solar radiation (*i.e.* the so-called “*water-leaving radiance*”) reflected by the open-surface water body under consideration, based on its “spectral characteristics” (*i.e.*, absorption, scattering and other relevant physical laws). The conceptual model exploits the causal links between the optical properties of the sensed signal and the inherent optical properties (IOPs) of the individual water-constituents. In practice, however, several additional factors present within the instantaneous field-of-view (IFOV) of the sensor (e.g., aerosols, atmospheric water vapor and gases) influence the satellite sensed (bulk) signal, which typically contains spectral contributions from these materials. These factors usually compounded the measurements and data interpretation. Therefore methods of signal correction and processing needed to be applied to the sensed signal to remove those disturbances in order to allow for the retrieval (extraction) of genuine ground spectra from the target object.

During recent years there has been a great deal of research devoted to building up new algorithms appropriate to overcome image processing difficulties and/or reconstruct the sensed signal ([4] [5]). Algorithms are now available that can be used for the extraction of lake water quality parameters (WQPs) from satellite images. Such algorithms are described in several publications (e.g., [6]-[9]). Several applications can be cited that have demonstrated their usability: [1] [6] [10]-[14].

This study was part of a research project aimed at developing a remote sensing approach towards the implementation of a GIS decision support system for the lake water management. The investigated WQPs are the three key model components for coastal waters ([15] [16]): 1) Chlorophyll-a (CHLa) [referred to as an index for phytoplankton biomass development]; 2) total ssuspended particulate matter (SPM) [taken as the dry weight of all suspended inorganic particles] and 3) colored fraction of dissolved organic matters (CDOM) [so-called “*yellow substances*”, consisting of aquatic humic and fulvic compounds, the presence of which has often been associated with acidic waters].

This paper reports on the preliminary results of investigations on the applicability of the commercially available MERIS image data for concentration retrieval of WQPs for Lake Guiers. The aim was primarily to employ this method as a reconnaissance tool for water quality monitoring and mapping of this shallow lake, using the FUB/WeW processor developed by ([14]). To date, research using this approach has focused essentially on lakes with greater extension and depth. Our specific objectives were twofold: firstly, the evaluation of performance of the FUB/WeW algorithm for signal correction of the raw MERIS scene (1b-image product level) and quantitative estimations of WQPs for the study lake; and secondly, to assess the variations in temporal features of the water quality in the lake and its dynamics based on a time series of WQPs estimates derived from the MERIS 2b-image end-product level. However, due to a lack of ground truths, background data from early studies were used to aid interpretation and tentative validation (*i.e.* calibration) of the derived WQPs data in this study.

2. Theoretical Concept

The conceptual model of the technique employed in this study relies on the relationship between the reflectance (R) recorded on board the MERIS-sensor and the inherent optical properties (*i.e.* IOPs or spectral characteristics) of the sensed open-water body. This relationship can be put in the form (e. g., [17]):

$$R(\lambda) = \gamma \cdot \frac{b(\lambda)}{a(\lambda) + b(\lambda)} \quad (1)$$

where $R(\lambda)$ is the spectral reflectance measured in band λ . The γ term is dependent on the directional illumination geometry of the light field emerging from the water body and may be expressed as ([18]):

$$\gamma = \frac{1}{1 + \frac{\overline{\mu_d}(\lambda)}{\overline{\mu_u}(\lambda)}} \quad (2)$$

where-in the term $\frac{\overline{\mu_d}(\lambda)}{\overline{\mu_u}(\lambda)}$ represents the ratio of the average cosine of the down-welling (incident) light to that of the up-welling light over the water body.

The term $a(\lambda)$ is the total absorption coefficient of the water body characterizing the decay rate of incident sunlight due to the process of absorption by the water molecules themselves and by the various suspended and dissolved components that have distinctive spectral signatures, and

$b(\lambda)$ is the total scattering coefficient of the water body representing the decay rate of incoming sunlight due to (back)scattering at the surface of these elements.

In Equation (1), each term is followed by the symbol for wavelength in parentheses (λ), since measurements are made in terms of monochromatic components. The components of absorption $a(\lambda)$ and $b(\lambda)$ thus symbolize the pooled spectral effects of both the water molecules and all water resident constituents on the incident sunlight reaching the target surface water body. Obviously, since the spectral properties of a reflecting medium relate to the specific inherent optical properties (IOPs) of its individual constituents, the per-unit concentration of the constituents and the coefficients $a(\lambda)$ and $b(\lambda)$ can be expressed as explicit functions that include the spectral properties of these constituents as follows (conjectural three components model for “*case-2 waters*”; ([15] [16]):

$$a(\lambda) = a_w(\lambda) + Pa_p^*(\lambda) + Ya_y^*(\lambda) + Sa_s^*(\lambda) \quad (3)$$

$$b(\lambda) = b_w(\lambda) + Pb_p^*(\lambda) + Sb_s^*(\lambda) \quad (4)$$

where the subscripts w , p , y and s refer to the optically active constituents (OACs) in the considered medium and stand for water, phytoplankton, yellow substances and inorganic ssuspended particles respectively, while the symbols P , Y and S refer to their respective concentrations.

In the notation used here, the asterisks denote specific coefficients of the components. For instance, $a_p^*(\lambda)$ refers to the specific back-scattering caused by phytoplankton in spectral band λ , while $b_s^*(\lambda)$ is the specific back-scattering coefficient of suspended particulate matter. Pure water forming a constant background optical property, its coefficients are written without asterisk.

3. Environment Setting of the Study Area

Lake Guiers is located in northern Senegal, lying between 15°35' and 16° Long.-W, and 15°50' to 16°35' Lat.-N (**Figure 1**). It is a shallow lake with a north-south elongation (about 50 km long and 2 to 7 km wide), and a maximum depth of 6 m in the central zone. It is an essential water resource for Senegal. It receives drain waters from the adjoining Senegal River at the border of Senegal with the Republic of Mauretania. The lake drains from north to south with maximum depths at the central zone, while the depth is shallower towards the southern end. It is in this inshore zone, which is partially exposed at low water that the lake discharges into the Ferlo valley, acting as the principal surface water outflow in addition to water losses from evaporation or vertical leakage to the underlying aquifer system.

Lake Guiers is bottoming at around -2 m below mean sea level and, at its highest mean water level (*i.e.* +4 m above mean sea level), it may expand to cover a surface area of about 320 km². Especially characteristic is the presence of aquatic plants (such as emerged/fixed and floating macrophytes) that populate the near shoreline (bank margins) environment, an area of very shallow water. These aquatic plants are important because they supply a local stabilization of the lake floor and act as trapping agents that allow suspended sediment to settle on the lake bottom and stabilize as soon as it is deposited. Moreover, they provide low energy wave action and surfaces for attachment or food gathering, and generate a good habitat for benthonic organisms. The offshore environment is the area of deeper water with a maximum water depth ranging from 4 m to 6 m. [19] describe this zone as an environment where uniform ecological conditions prevail which provides an optimum environment for algal growth. There is a tendency for phytoplankton to locally develop from the low-water shoreline environment to the offshore environment. The growth density of the principal living organisms is related to water depth and movement, and their distribution defines three distinct ecological zones (see **Figure 1**), namely

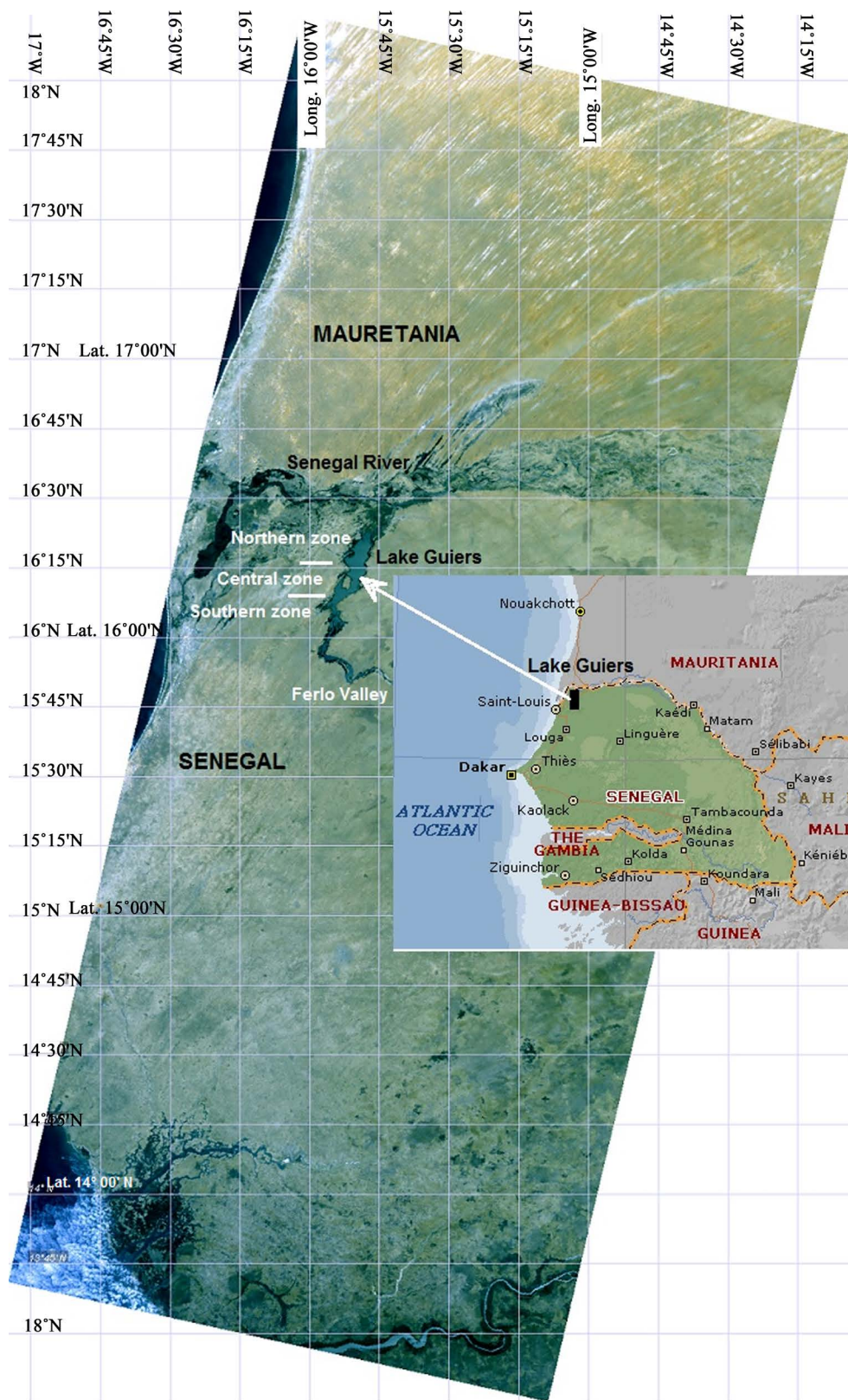


Figure 1. Coverage area of the April 27th, 2007 MERIS FR 1b-composite image showing the location of the study area within Senegal (flow is from east to west for Senegal river and north to south for Lake Guiers).

northern, central and southern zones. However, in the typhae-dominated southern zone and alongside the bank margins, the occurrence of CHLa, in terms of primary production (algal activity), may be low due to the high competition exerted by the macrophytes vegetation.

Initially, the hydrological regime of Lake Guiers was subjected to the natural fluvial dynamics of the Senegal River. Nowadays, the regulating dams constructed on the river, as well as the channelization of the river, make possible a large-scale storage and use of river water independent of natural flooding. Before any regulation was attempted, the hydrology and hydrochemistry of the lake were characterized by major consequences on the hydrophytes settlements, due to the phases of alternating high and low water levels (*i.e.* drought events) and accompanied high salinity. [20] and [21] found that the new hydrological conditions generated by the regulating dams (*viz.*, the stabilization of the lake stage at fairly constant elevation of 2 m above mean sea level (see **Figure 2**) and, hence, the permanent softening of the lake water quality) are ecological factors that encouraged the expansion of an important aquatic vegetation of free floating and fixed macrophyte (essentially *Typha*, *Phragmites*, *Pistia stratiotes*, *Echinochloa* and *Nymphaea*). According to [22], this proliferation of aquatic plants best explains the rapid spread of *schistosomiasis*, the larval forms of parasitic blood flukes that currently affect the health of populations living in lakeside villages.

Lake Guiers' main uses are domestic, agricultural, industrial water supply and fisheries. Its water supply accounts for nearly 60% of the daily water consumption of the capital city of Senegal (Dakar) and its suburbs. However, due to its surrounding fertile soils, irrigation agriculture within the lake catchment is increasingly impacting on the water quality, the extent of which is not well documented. The area is characterized by the extension of relatively flat and open landscapes of SW-NE trending sand dune systems (*i.e.* Quaternary ergs) overlying the Tertiary substratum. The lake bed geology, as described from a series of cores to a depth of 5 m, grades downwards from bluish-green colored silts to fine sand sediments ([23]). The climate is arid (Sahelian type), with almost all of the annual precipitation (average: 300 - 400 mm/yr) occurring during the rainy season which lasts from July to September. Vegetation is of the savannah type, namely tiger bush, interspersed with bare soil and agricultural fields. A mean annual air temperature of about 26.3°C (min: 12°C, max: 42°C), with small deviations in monthly mean temperature, reflects the proximity of the sea. The amplitude of variations does not exceed $\pm 5^\circ\text{C}$, with the hottest months being from May to October. The area mostly experiences north-easterly Saharan trade winds (Harmatan) of 2 - 6 m/s monthly mean.

4. Background Information

The lake waters are of pH 6.8 to 9 and vary seasonally in temperature between 18°C and 30°C (with a mean 25°C). Amplitudes of the daily temperature variations of the waters rarely exceed 5°C. Differences in temperature between the top and bottom water layers are in range 4°C - 5°C or less, with the greatest variation occurring in the period of December to March according to [24]. Data from this study indicate electrical conductivity in the range of 160 - 210 $\mu\text{S}/\text{cm}$ (period 2002-2004), total dissolved solids in the range of 198 - 250 mg/L, with

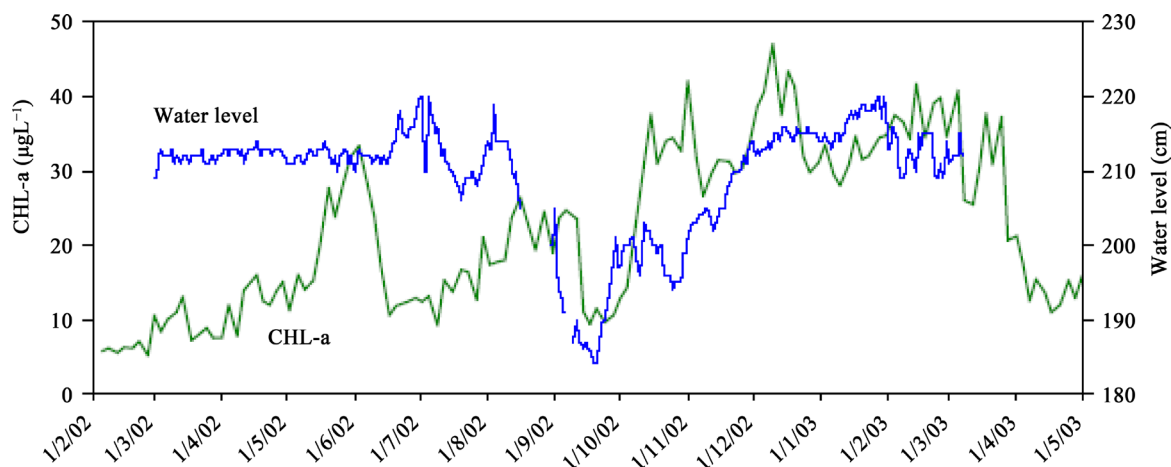


Figure 2. Pattern of variations of Lake Guiers CHLa contents and water level in the observation period February 2002-May 2003 (modified after [19]).

Ca^{2+} , Na^+ and HCO_3^- and Cl^- being the dominant ions, while nutrients PO_4^{3-} and NO_3^- are in the range of 0.2 - 1.8 and 0.2 - 2.5 mg/L respectively. The oxygen saturation typically is above 60%. Under these conditions, the euphotic layer of the lake almost matches the entire water column. Environmentally, this means very uniform ecological conditions which provide ideal circumstances for phytoplankton development.

Up till now, the only literature available on the lake's water quality generally focused on the occurrence of CHLa and SPM (e.g., see [19] [24] [25]). However, little is known about the occurrence of CDOM. [19] measured CHLa contents in the range of 5 to 47 $\mu\text{g CHLa L}^{-1}$ and suggested a sort of seasonal trends (as presented in Figure 2) which might be related to phytoplankton biomass variations. However, this may not be considered a regular/cyclic pattern, as evident from the comparison of CHLa occurrence for the periods of February-April, 2002 and February-April, 2003. Similar results was obtained during the winter months by [25], who noted the occurrence of higher CHLa contents (45 - 70 $\mu\text{g CHLa L}^{-1}$) as an obvious and characteristic effect of temporal phytoplankton variations.

A similar scenario was observed for SPM concentrations by [25], with values in the range 15 - 45 $\text{mg}\cdot\text{L}^{-1}$ (mean 29 $\text{mg}\cdot\text{L}^{-1}$). His Figure 3 ([25]) presents evidence of a declining water turbidity during the period May-September 2005. SPM values are lowest in the period of July-August, a trend that is consistent with the seasonality of the climate as discussed further below. SPM concentrations increase steadily for the rest of the year to reach the maximum peak in February-March. The SPM values of [25] are somewhat higher than those reported by [26] along an N-S transects of the lake, with values of 3 to 30 mg SPM L^{-1} (average 13 mg SPM L^{-1}). The [26] measurements were lowest in the northern ecological zone, with values of 3 to 10 mg SPM L^{-1} , and which increase towards the thicker central portion of the lake, reaching values of up to 30 mg SPM L^{-1} . Toward the south, the SPM concentration values decrease again, a situation that can be attributed to the presence of macrophytic vegetation that incidentally decreases the hydrodynamic conditions and thus favoring particle sedimentation. However, SPM concentrations as high as 30 mg SPM L^{-1} may occur also in the southern shallow water zone of the lake as well, as observed by [26] at downstream section of the lake, near Keur Momar Sarr embankment. The probable explanation is a sporadic change in turbidity due to water agitation or particles input from desert sand storms. Apparently, some patterns of spatial and temporal variations of the SPM concentrations were suggested by the various authors, which probably indicate some characteristic features that typify the lake behavior. Evidence comes from the fact that the SPM load of the lake usually decreases during the summer months with the onset of the rainy season. This is as a result of the episodic effect brought about by the seasonal changes in wind direction, as monsoon airstreams blow onto the land, thus supplying the trocken Saharan trade winds (harmattans). In the seasonally warm periods (*i.e.*, mostly during the months of February and March) sand particles input into the lake waters is created by the large dust storms from the Sahara Desert. Strong winds that carry desert dusts into the atmosphere are consistently produced every year as the air over the hot desert regions is heated and expands in volume causing it to rise upwards.

Another important feature of the lake waters reported by [24] during the period 2002 to 2005 is the presence of high phytoplankton biomass (with a pluriannual average value of about 46 $\mu\text{g CHLa L}^{-1}$) that immobilizes most of the nutrients in the lake. According to the author, cyanophytes and chlorophytes dominated the phytoplankton community of the lake during the period, with yearly averaged biomass productivity as 6.5 mg C (mg

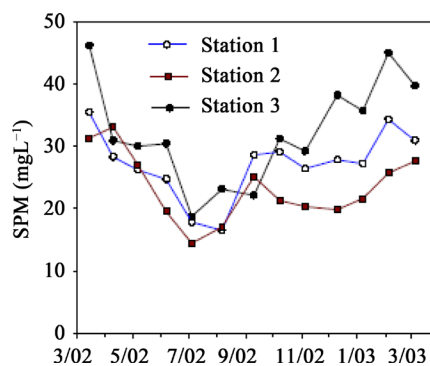


Figure 3. Pattern of variations through time of SPM concentrations in Lake Guiers for the observation period from March 2002 through March 2003. Note: SPM concentrations shows similar variation at the three stations, with values in range of 15 - 45 $\text{mg}\cdot\text{L}^{-1}$ ([25]).

$\text{Chla}^{-1}\cdot\text{h}^{-1}$. During this observation period, the CHLa content of the lake waters varied with yearly averages of about $20 \mu\text{g CHLa L}^{-1}$ in 2002, $18 \mu\text{g CHLa L}^{-1}$ in 2003, $28 \mu\text{g CHLa L}^{-1}$ in 2004 and $51 \mu\text{g CHLa L}^{-1}$ in 2005.

Therefore, judging from the broad range of CHLa values (from 5 to $70 \mu\text{g CHLa L}^{-1}$) reported by the various researchers ([19] [24] [25]), one may conclude that Lake Guiers' trophic index may vary appreciably, almost from oligotrophic to eutrophic state. It must be emphasized that the applied margin of safety for lake water is CHLa concentrations about $\leq 9 - 10 \mu\text{g}\cdot\text{L}^{-1}$; this is because taste and odor problems begin once the chlorophyll-a concentrations reach higher values. For biota and others hydrophobic organic substances in lake waters, the EU fresh water quality standards with reference to SPM is 15 mg/l.

5. Database and Methodology

MERIS products are satellite image data acquired by the Medium Resolution Imaging Spectrometer (MERIS) on board the European Space Agency (ESA) Environmental Satellite (ENVISAT)-1 launched on March 2002. MERIS is a typical nadir-looking push-broom imaging system that enables monitoring of the Earth's atmosphere and surface with a repetition time of 3-day intervals. It can be operated either in direct mode (so as to deliver a full-resolution-FR product of 300 m on-ground resolution) or in averaging mode (so as to produce a reduced resolution-RR product of 1200 m on-ground resolution). The MERIS sensor operates with 15 programmable bands in the spectral range 412.5 - 900 nm, with a 10 nm average bandwidth. Further details on the instrument are reported in [27].

The MERIS data used in this study were provided by the TIGER project N° 2793 on behalf of the ESA, and covers the observation period from 2003 to 2010. Most observations were concentrated on the months of January, March, April, May, August, October and November. The average monthly mean concentrations were then calculated for each estimated parameter based on the sensor's effective repetition rate of 3-day intervals (*i.e.* using the 9 - 10 scenes or so taken during the month). The calculated monthly mean concentrations were subsequently averaged per annum, and then averaged over the observation period (*i.e.* 2003-2010) to yield the long-term (pluriannual) mean for each parameter.

The studied scenes comprised a set of rough MERIS full resolution 1b-image product-levels and another set of 2b-image end-product levels. The focus of the methodological approach was:

- Objective 1: to test the suitability of the FUB/WeW algorithm ([14]) for signal correction and concentration estimates and mapping of the lake WQPs using the rough 1b-image product, and
- Objective 2: to demonstrate the potential use of the 2b-end-products (*i.e.* on board ENVISAT-1 already processed images) for changes detection.

Objective 1 was addressed by selecting the image presented in **Figure 1**. This image taken on April 27th, 2007 was the only cloud-free scene covering the study area out of a set of ten 1b-scenes available for purchase in Phase I of this research project; the remaining scenes had intolerable levels of cloud cover. The processing method using the MERIS FR 1b-product as input for the FUB/WeW algorithm has been presented elsewhere ([28]).

In contrast, cloud cover was not a primary limitation for Objective 2, which was an application based on the standard MERIS FR 2b-end product level. These are “*ready-to-use*” image data that offer the opportunity of straightforward visualization of the generated WQPs using the BEAM (BASIC ERS & ENVISAT (A)ATSR and MERIS)-VISAT software. The BEAM-VISAT Toolbox developed by Brockmann Consult for ESA (see [29] for more details) enables viewing of the output quality products (*i.e.* physical parameters) contained in the level 2b-product. The BEAM-VISAT version used here is Version 4.8 (<http://www.brockmann-consult.de>).

Finally, it should be pointed out that surface water quality mapping based on MERIS FR images typically represents a ground-based sampling on a 300m-by-300m grid cell basis as the smallest unit area (namely, the image pixel size). Each grid cell (or pixel) is assigned a parameter value averaged out over its area.

6. Results and Discussion

6.1. Description of the FUB Model Results

Table 1 presents the summary statistics of the pixel values for the three WQPs derived from the April 27th, 2007 MERIS FR 1b-product level by applying the FUB algorithm, while **Figure 4** shows their frequency distributions (FD) along with fitted normal distribution model curves $N[\mu, \sigma]$, wherein the symbols μ and σ represent, respectively, the mean and standard deviation of a given parameter respectively.

Table 1. Statistical summary of the retrieved concentrations values for the three analyzed WQPs.

Parameter	SPM	CDOM	CHLa
	(mg·L ⁻¹)	(m ⁻¹)	(µg·L ⁻¹)
Sample size	1151	1147	877
Mean (average)	22.03	1.33	62.13
95% conf. int. (mean)	±1.4%	±1.1%	±1.3%
Median	22.99	1.31	60.54
Mode	22.81	1.29	58.32
Geometric mean	19.79	1.33	60.96
Variance	28.07	0.01	158.85
Standard deviation	5.3	0.11	12.6
Standard error	0.16	0	0.43
Minimum	0.17	1.1	32.36
Maximum	28.92	1.88	117.58
Range	28.75	0.77	85.23
Lower quartile	22.18	1.27	55.24
Upper quartile	23.79	1.37	67.2
Skewness	-2.78	1.94	1.28
Coeff. of variation	24.04	8.53	20.29

As shown in **Table 1**, the respective mean, median and mode for SPM, CDOM and CHLa are close enough as to reasonably corroborate the standard assumption for normal distribution. Moreover, the statistics indicate a 95% confidence interval on mean concentration values in extremely narrow ranges (*i.e.* from ±1.1% to ±1.4%), thus suggesting a high probability for an efficient estimate of the hypothetical “population mean” for each parameter.

Close inspection of the range of mean values reported in **Table 1** reveals that the average concentrations of all three WQPs exceed the limits of drinking water regulations, suggesting poor quality waters within the lake compartments at the time of image acquisition. CDOM values have a moderately lower coefficient of variation (8.53%), compared with CHLa and SPM values with 20.3% and 24%, respectively; this can be attributed to the fact that CDOM are miscible constituents and thus may be distributed homogeneously within the lake waters. However, CHLa and SPM constituents are present in the water medium as suspensions and, therefore, may exhibit higher spatial variability due to the complexity of the lake ecosystem in terms of structure and physiography.

6.1.1. Comparative Assessment

CHLa values: At least two major peaks (one at around 62 µg CHLa L⁻¹ and another at about 72 µg CHLa L⁻¹) can be noticed in the frequency distribution (FD) of CHLa (**Figure 4(a)**), which indicates mixed feature or spatial variability of the CHLa concentrations. CHLa values inferred for pixels located along the bank margins are fairly high (>80 µg CHLa L⁻¹), resulting in the chlorophyll pigment production from the macrophytes vegetation populating the near-shore zones of the lake. Moreover, the 95% confidence interval, involving the mean for CHLa, from 61.32 to 62.94 µg CHLa L⁻¹, is within narrow limits. This means that if the retrieved CHLa values are averaged to symbolize the standard trophic state of the lake at the time of satellite overpass, then the lake status can be deemed “eutrophic” with a 95% probability at that moment. This is consistent with field observations from early studies ([19] [24] [25]).

SPM values: The frequency curve for SPM (**Figure 4(b)**) exhibits two dominant peaks, the first at about 25 mg·L⁻¹, and the second at about 29 mg·L⁻¹. This also suggests a mixed feature and variability in the turbidity level of the lake water. However, the distribution pattern reveals that SPM values have roughly three population groupings. The fitted normal distribution curve is skewed to the left indicating that most SPM values are “larger” than the mean value of 22.03 mg·L⁻¹. This means highly turbid conditions throughout most parts of the lake, a finding that is consistent with similar results previously obtained by other investigators (e.g., [25]). It could be

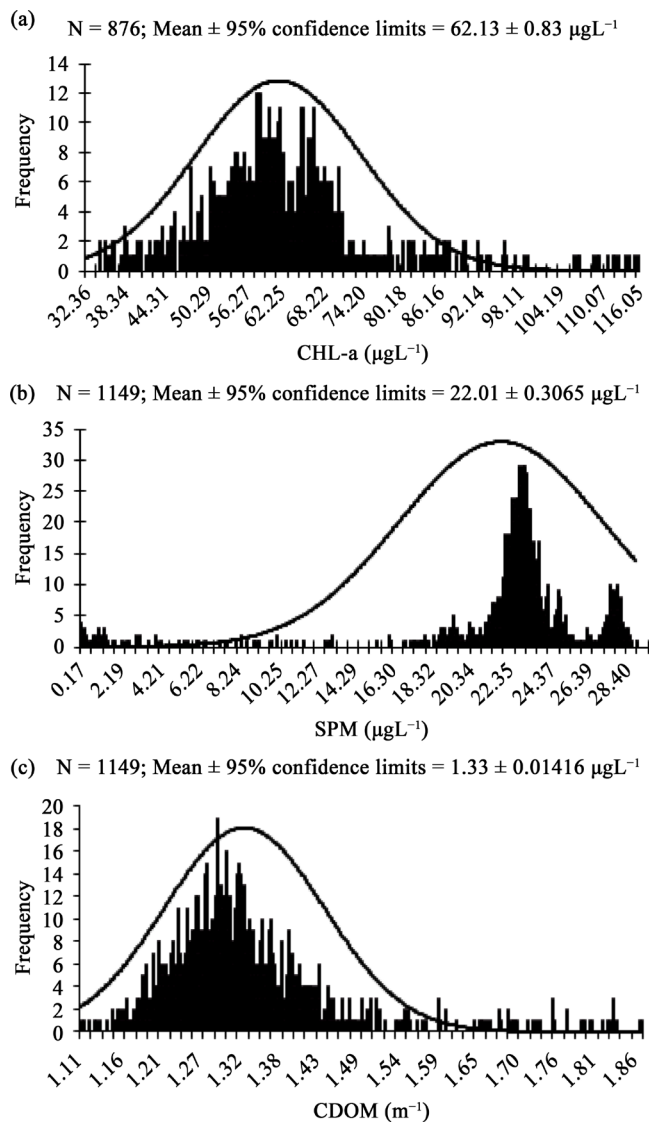


Figure 4. Frequency histograms with fitted normal distribution curve for (a) CHLa values (b) SPM values and (c) CDOM values.

inferred that the apparently high turbidity level of the lake could be the result of a variety of factors, including, for example: sand particles input from Saharan dust storms that are predominantly active during the period of the year in focus (April month); contributions from feeding river waters (as the sediment-laden streams water flow into the lake); and the effect of high-speed Saharan trade winds that typically induce wave motions and bottom particle re-suspension within shallow water depths.

CDOM values: The histogram plot of the CDOM concentration values (**Figure 4(c)**) indicates a fairly unimodal distribution due to a smaller variance (see **Table 1**). There is no literature data on CDOM available for making comparisons with the FUB-predicted values. However, the observed lower range of 0.77 CDOM m^{-1} (with measurements ranging from 1.105 to $1.877 \text{ CDOM m}^{-1}$) is consistent with similar narrow ranges and orders of magnitudes reported in the hydrological literature ([30] [31]).

As part of further data evaluation, the studied WQPs are expressed in terms of contoured concentration maps as presented in **Figure 5** where the variability in colour is related to concentration variations. Visual inspection and assessment of the spatial variability revealed a general westward increase in CHLa and CDOM concentrations as against the SPM concentrations. High CHLa and CDOM concentrations and low SPM concentrations in the western shoreline are thought to result from the occurrence of the macrophytic vegetation on the lake reaches.

Moreover, the highest SPM concentrations are found upstream (near the Mbane village) and downstream of the lake (near the Sear village). Compared to the central zone, these are locations where the lake is shallower and/or narrower, *i.e.* places where the lake hydrodynamics, and wind-induced particle re-suspension effects, are more important. The spatial variability in the SPM concentrations observable in **Figure 5(c)** in the N-S direction of the lake is consistent with the one depicted in previous studies ([24] [26]).

6.1.2. Correlation Analysis

Figure 6 shows a tentative correlation between FUB-predicted SPM values and early *in-situ* measures compiled from the literature ([26]). With knowledge of the geographic coordinates of the locations of these field measurements, it was possible to locate and spatially match-up the *in-situ* measurements with SPM values retrieved from the MERIS 1b-image at corresponding pixel positions.

The best correlation coefficient, $r = 0.741$ ($R^2 = 0.5491$) obtained by discarding one outlier data point, is not statistically significant at the 95% confidence level (ANOVA P-value = 0.0567), suggesting a poor linear

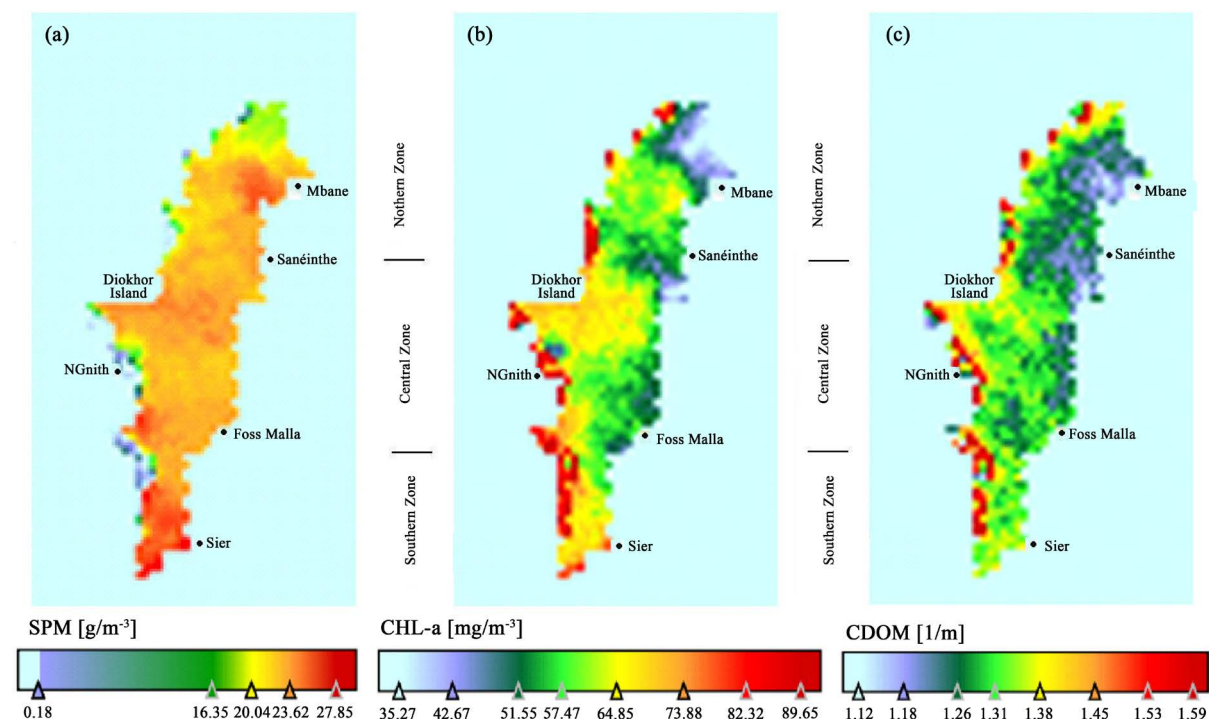


Figure 5. Spatial distribution of SPM (a), CHL-a (b) and CDOM concentrations (c) in Lake Guiers waters based on FUB algorithm retrieval from the April 27th, 2007 MERIS observation.

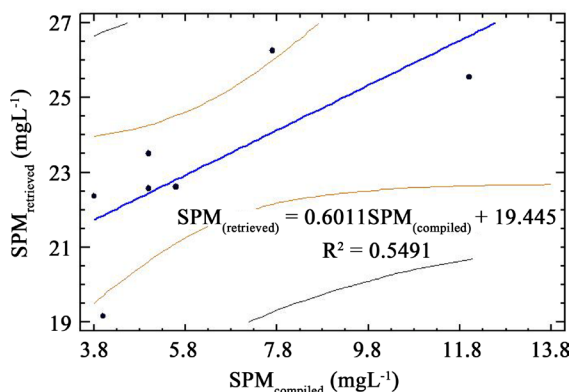


Figure 6. Plots of FUB-predicted SPM values versus SPM values measured by ([15]).

relationship between the two data sets. However, nearly 55% of the variance of FUB-derived SPM values could be explained by the fitted line, judging from the coefficient of determination R^2 . This result increases the confidence level in the reproducibility of the data. Nonetheless, it is possible to infer that real-case regression equations derived from comparing FUB retrievals to ground truths might provide a basis for reliable WQPs estimates.

In addition, assessment of the possible relationship between CHLa and CDOM concentrations as presented in **Figure 7**, revealed a correlation coefficient (r) of 0.686 ($R^2 = 0.4709$), which is statistically significant at 0.05 level (ANOVA P-value = 0.0000). This signifies that nearly half of the variance of the CDOM absorption can be explained by the variance of the active phytoplankton biomass. Presumably, the implication is that the degradation of phytoplankton cells within the system accounts for a CDOM proportion of 47%.

However, the remaining 53% proportion of CDOM that cannot be explained by the fitted equation may be related to an “*allochthonous*” source which, in turn, may explain the markedly high CDOM contents in the lake. Other factors, which may influence the CDOM, include natural cycling of elements (through the decay of plants and phytoplankton) and direct anthropogenic activities such as agricultural practices and industrial wastewater inputs.

Figure 8 displays the correlation between CHLa and SPM values with a huge point scattering with respect to the best-fitted line ($SPM = -0.1729 \text{ CHLa} + 32.059$). Obviously, about 18% of the variance of SPM values can be explained by the fitted equation, with a correlation coefficient (r) of 0.425. This is a poor negative correlation which is statistically significant at the 5% level (ANOVA P-value = 0.0000), suggesting possible inverse relation between CHLa and SPM values. High CHLa values ($>70 \mu\text{g CHLa}\cdot\text{L}^{-1}$) basically outweigh the slope of the fitted regression line. Nonetheless, a closer visual examination of the plot revealed that SPM concentrations are generally found to decrease with increasing CHLa concentrations under two different scenarios:

Scenario A: At higher CHLa concentrations, which typically indicate chlorophyll pigment production from macrophyte vegetation, the apparent inverse relationship with SPM can be attributed to the reduced hydrody-

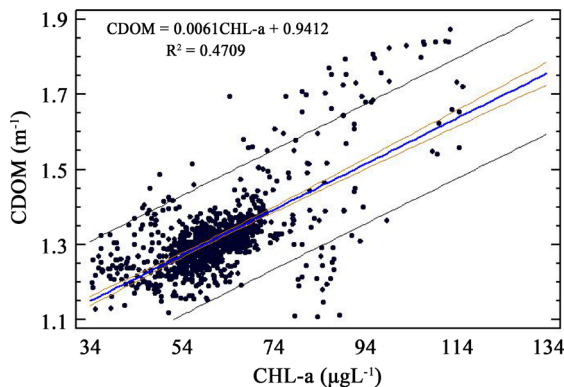


Figure 7. Relationship between CDOM concentration and CHLa concentration.

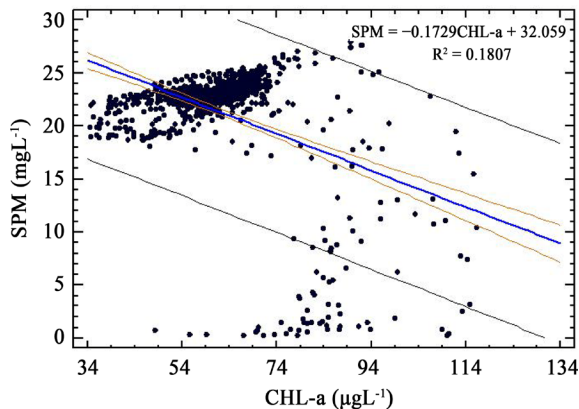


Figure 8. Relationship between SPM concentration and CHLa concentration.

namic conditions, which favour sedimentation of suspended particles under such macrophyte-dominated subsystems. This is consistent with the low SPM concentrations in places with dense aquatic macrophytes development as reported in [26].

Scenario B: In macrophyte-dominated subsystems, the fact that phytoplankton is of minor importance, as reported in [31], clearly supports the higher CHLa values ($>70 \mu\text{g CHLa L}^{-1}$). Thus, this explains the relatively weak positive correlation of the data points with SPM at much lower CHLa values.

6.2. Change-Detection Study

Understanding the lake's dynamics is an important issue for the lake waters management. However, it was not possible to critically examine this issue in this study due to lack of background information. In fact, the methodology requires the need to address the driving forces that affect phytoplankton growth rate that might have an impact on CHLa concentrations. The approach should also take account of the different causes of lake water turbidity, as well as the sources and mechanism of particles input. Many eutrophication models ([32] and [33]) have demonstrated the role of water temperature, intensity of sunlight and nutrients dynamics for phytoplankton growth. However, a high growth level also requires reduced water movement (*i.e.* quiet flow conditions). This is because under high flow, a turbulent hydrologic regime may develop, resulting in turbid waters and strong bottom-water currents that fall into intolerable limits for algal biomass development. Turbidity mainly comes from feeding runoff river water streams that carry large amounts of bed- and suspended-load solids into the lake. This may also possibly originate from sand particles introduced to the lake by Saharan sand storms and particles re-suspension due to bottom currents. As part of Objective 2 the following tentative interpretation was made from a chronological series of MERIS 2b-image products, based on these sources.

Long-range forecasting: Long-term mean-concentration values that would provide indications on the lake dynamics over time are presented in **Figure 9**. They range from 2.22 to $23.7 \text{ mg}\cdot\text{L}^{-1}$ for SPM, 0.134 to $29.3 \mu\text{g}\cdot\text{L}^{-1}$ for CHLa and 0.081 to 0.447 m^{-1} for CDOM. These values are within the range of those sampled from the MERIS 1b-product level. Based on the differences in pixel color, it is possible to suggest that SPM concentrations are highest where fairly high energy conditions prevail (**Figure 9(a)**), viz., in the feed-water entrance of the northern zone, along the eastern near shoreline bank, and the central off-shore zone. These are places where turbidity currents and bottom currents dominate the lake hydrodynamics. In contrast, the lower SPM estimates obtained downstream, in the barrier islands protected southern inshore zone and along the western margins, are attributed to the possible influence of the vegetation. Indeed, the aquatic plants invading these shallow water environments decrease the hydrodynamic conditions, thus allowing suspended sediment to settle. These low energy environments where algal growth might be favoured, are seen (**Figure 9(b)** and **Figure 9(c)**) to exhibit the highest CHLa and CDOM values, yielding maximum pluriannual means in the ranges $23 - 29 \mu\text{g}\cdot\text{L}^{-1}$ for CHLa and $0.294 - 0.447 \text{ m}^{-1}$ for CDOM. The correlation between these two parameters is reflected in the similarity of their geographical distribution pattern as shown in **Figure 9(b)** and **Figure 9(c)**.

When examined in detail, algal production occurs mainly on the inner zone and on the barrier island protected southern ecologic zone (**Figure 9(b)**). As explained earlier, the high CHLa level in these environments, and its correlation with CDOM level, is believed to be partly related to the parallel process of biomass reduction (mineralization) as algae decay and, to a certain extent, other processes like plant decay or anthropogenic activities.

Seasonal forecasting: Assuming that changes in the WQPs concentrations come from temporal changes in the driving environmental factors, a change-detection was assessed for the period 2003 to 2010 by comparing monthly trends. In this respect, **Figures 10-12** show co-extend WQP concentration maps of the monthly mean estimates averaged on the monthly scale for six selected months, starting on January each year, with an intervening interval of one month. The comparison demonstrates the general characteristics of the seasonal variability for each WQP. It can be seen that SPM contents are highest around the month of March (**Figure 10**) when dust storms from the Sahara Desert are active, and during the rainy period (*i.e.* August) as turbid runoff river water, that carries a large amount of bed- and suspended-load, flows into the lake.

As may be seen also from **Figure 11** and **Figure 12**, CHLa and CDOM were estimated to show a similar pattern of seasonal variation within the lake compartments, suggesting a related mechanism of origin. The distribution trend revealed increasing concentration values during the months of March, October and November. However, the month of November exhibited the highest CHLa concentrations, while CDOM revealed highest contents on March. This is the period when SPM values are highest (see **Figure 10**), that is, when turbidity conditions

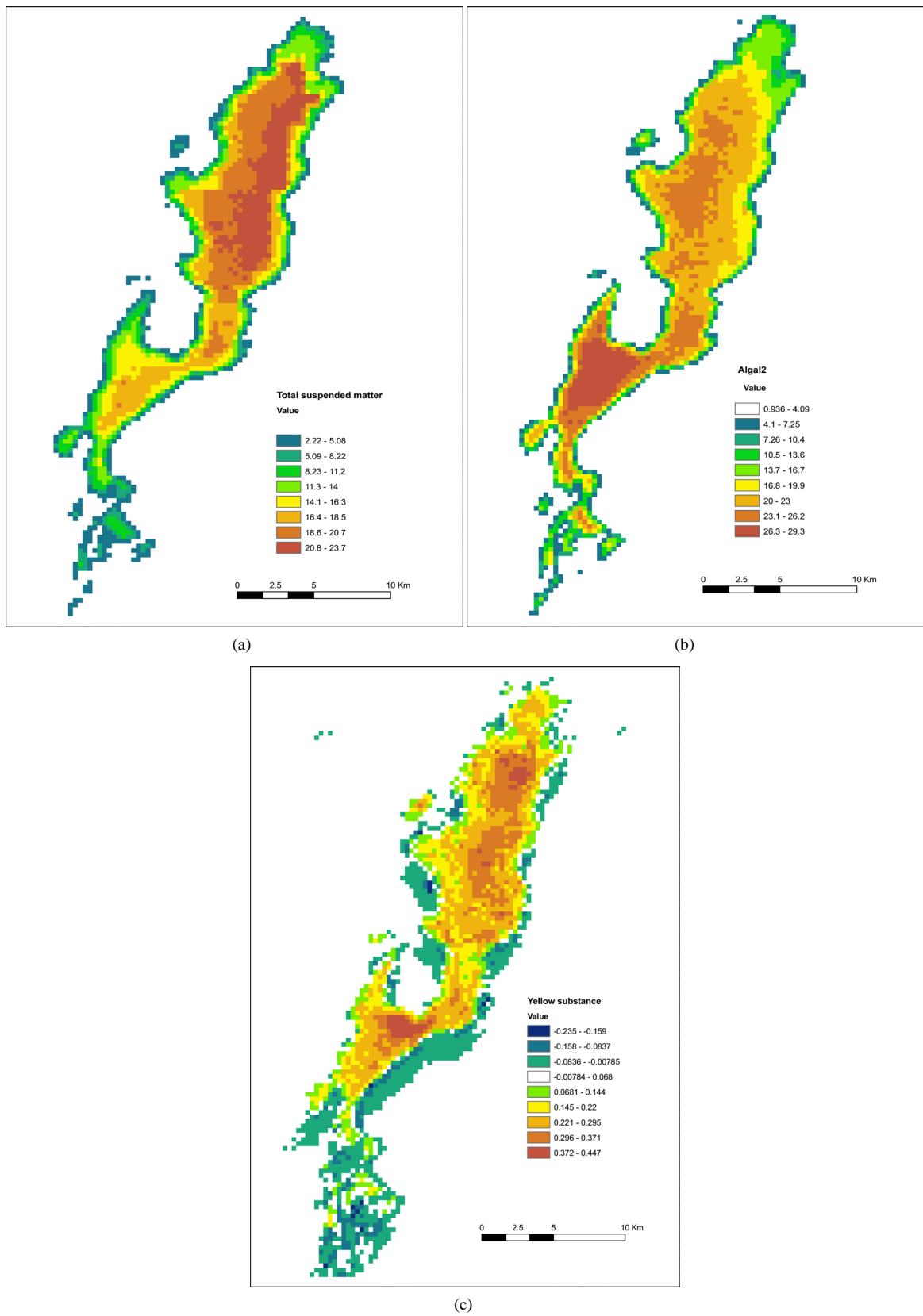
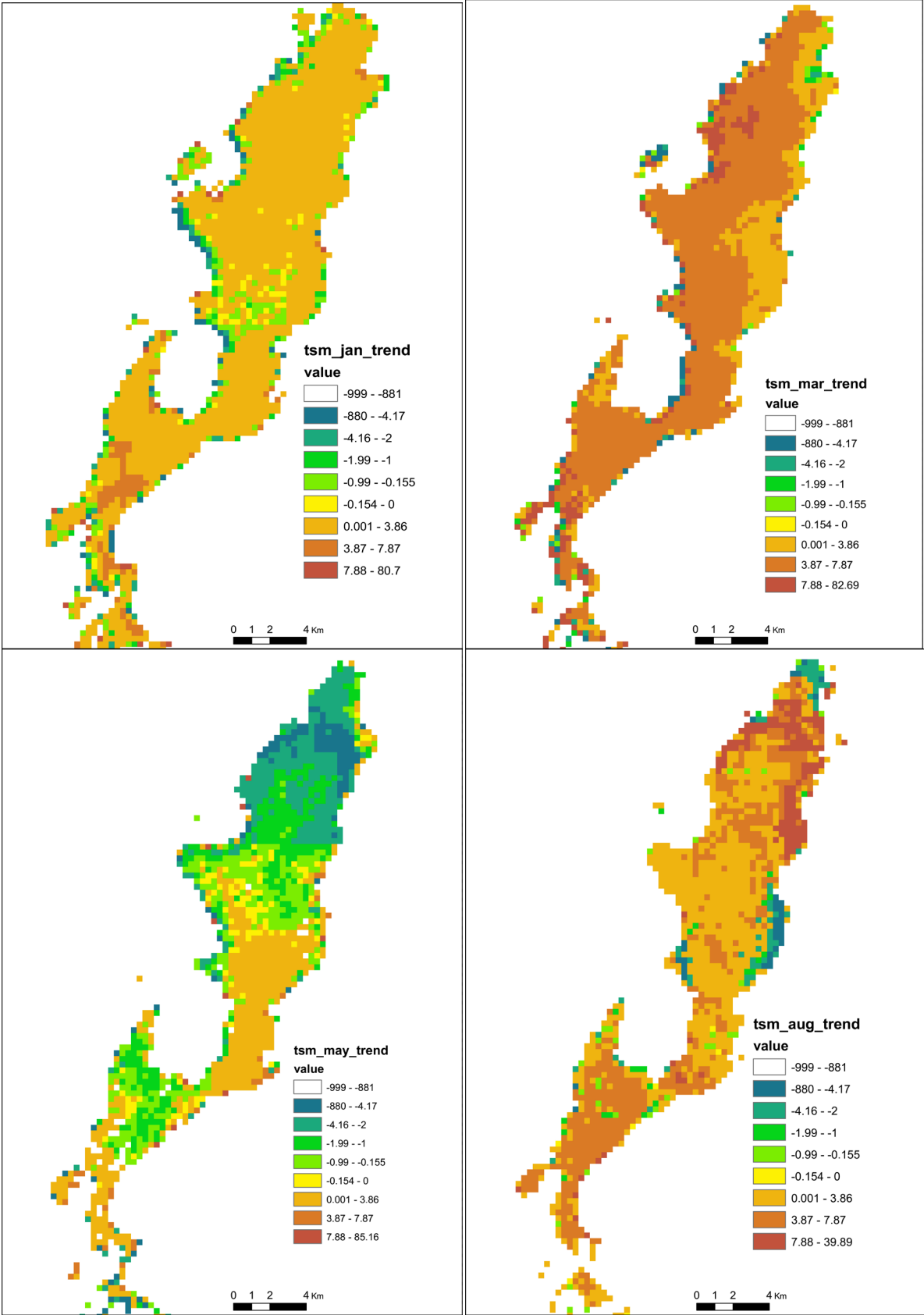


Figure 9. Average pluriannual mean concentrations of the WQPs: (a) SPM; (b) CHLa and (c) CDOM (Period 2003-2010).



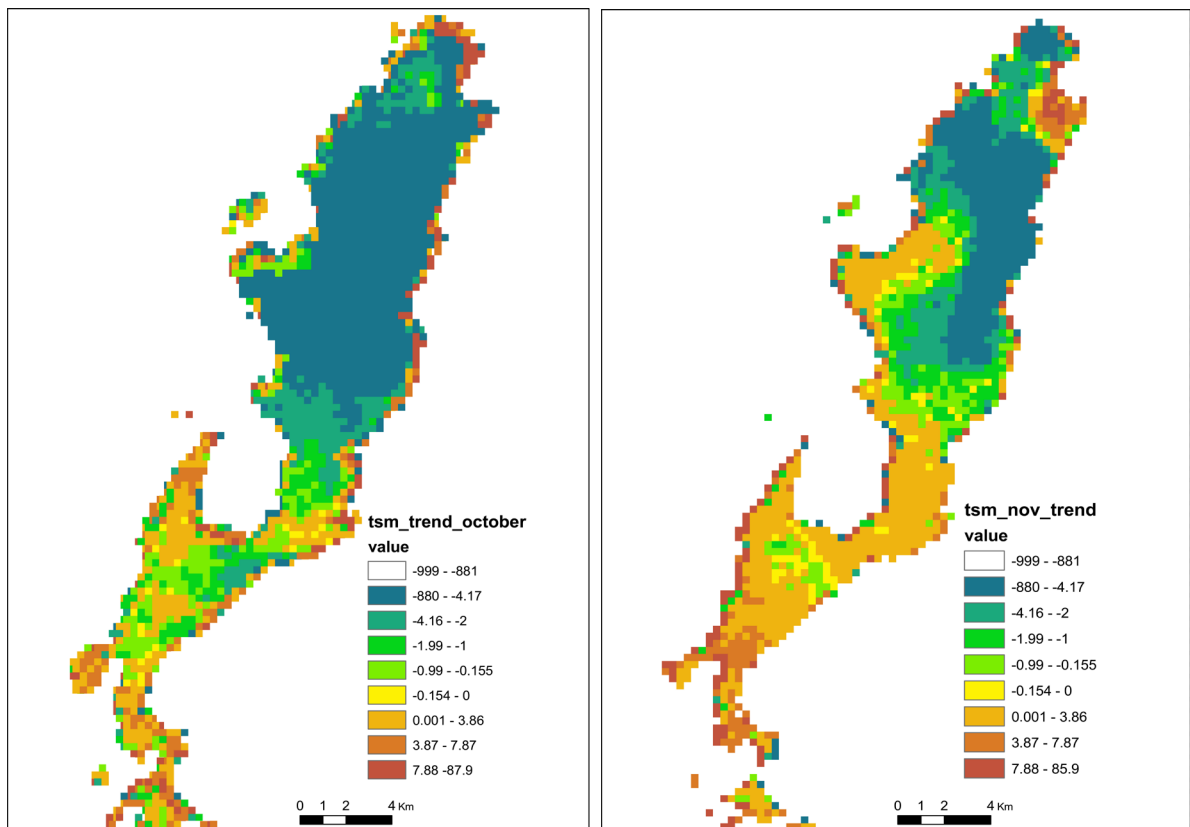
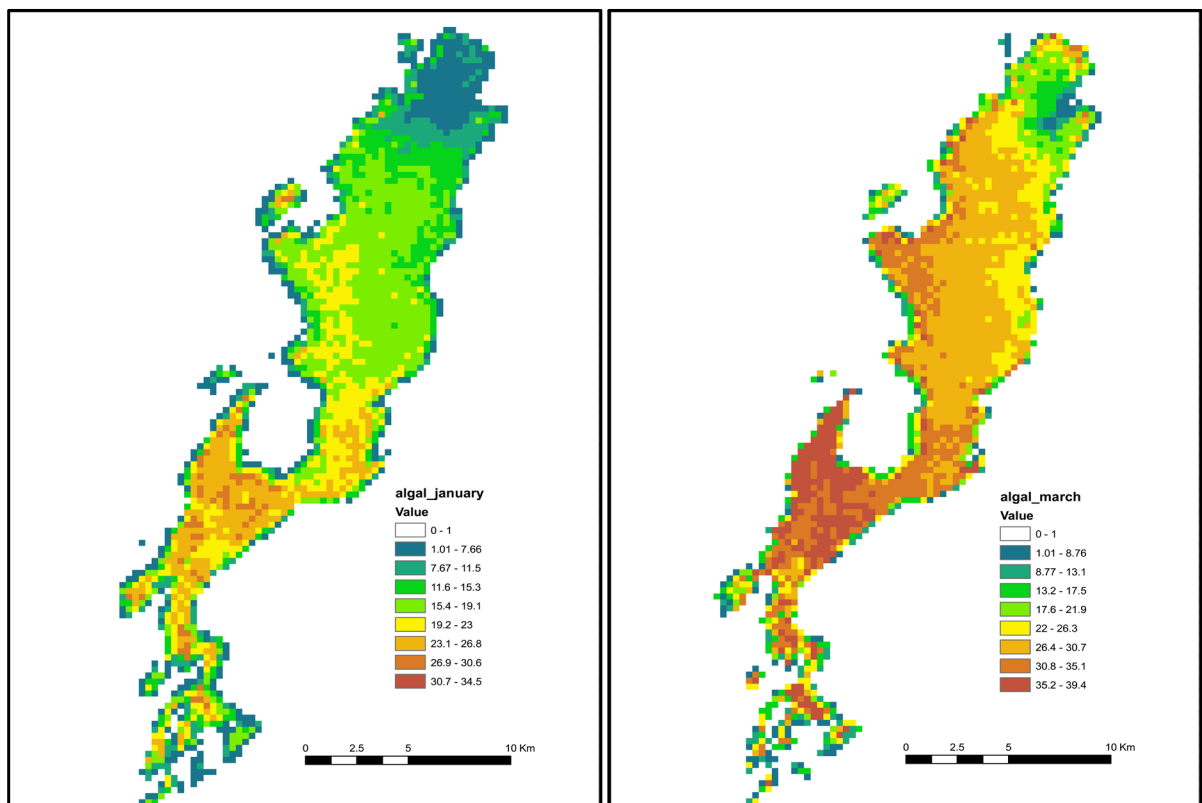


Figure 10. Mean monthly spatial distribution of SPM (period: 2003-2010).



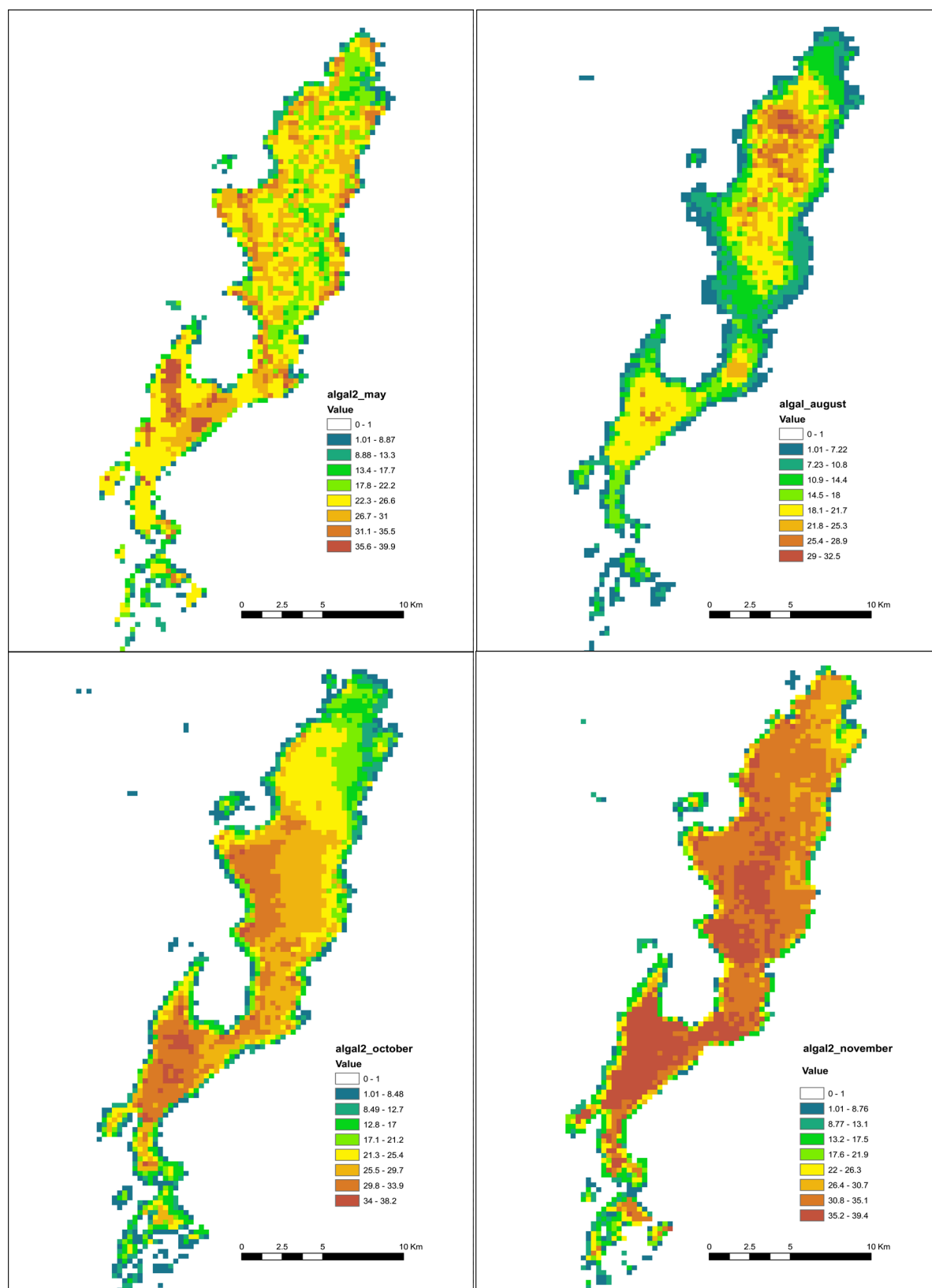
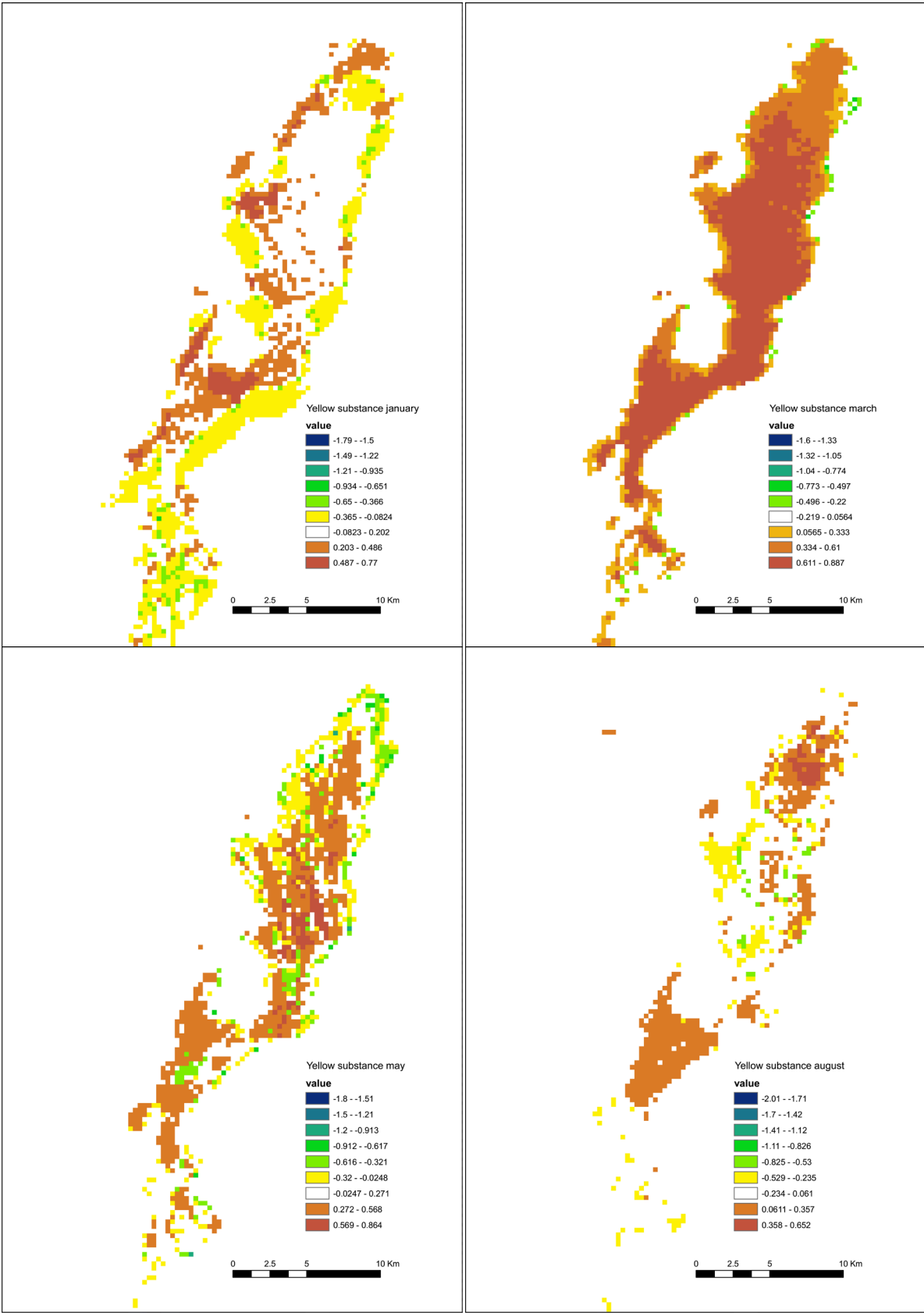


Figure 11. Mean monthly spatial distribution of CHLa (Period 2003-2010). Note: the comparison shows the November month with the highest abundance estimates of phytoplanktonic organisms.



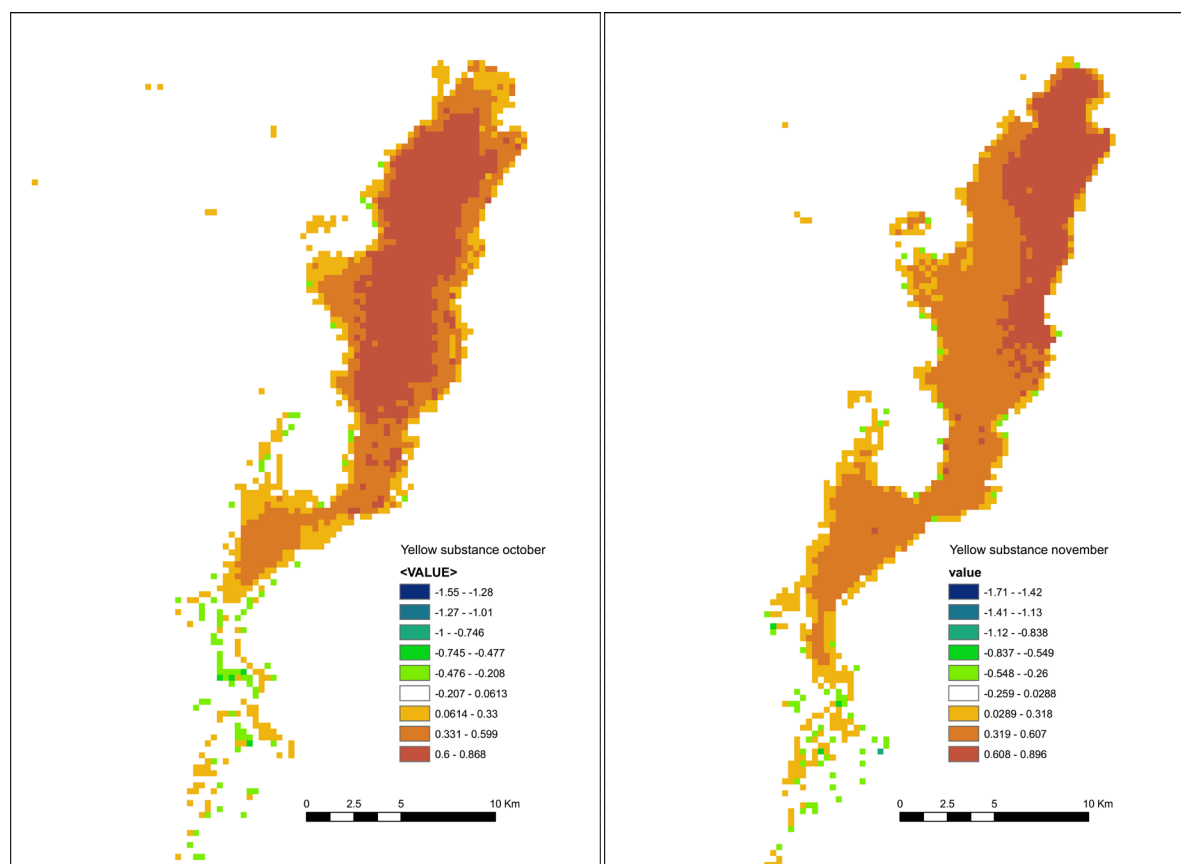


Figure 12. Mean monthly spatial distribution of CDOM (period 2003-2010).

might be environmentally so critical that algae may decompose and result in an abundant presence of CDOM. Nonetheless, the minimum concentration for both CHL_a and CDOM in the winter month of January suggests the reduction of algal activity as soon as water temperatures are lower.

7. Summary and Conclusions

This study examined the feasibility of applying MERIS imagery for a synoptic monitoring of the water quality of Lake Guiers, an important surface water resource for Senegal. Based on the application of a chronological data series of MERIS 1b- and 2b-image product levels as input data into the “easy to use” BEAM-VISAT software, the concentration of three main parameters relevant for the lake’s water quality management was extracted. The values calculated as part of this study matched well with literature data, thus supporting our hypothesis for the capability of this method to provide reasonably valid estimates. Moreover, some characteristic seasonal changes that occur in the lake were recognized and then discussed based on background information. However, an effective assessment of the accuracy of such estimates, and validation of the applicability of the method, warrants the need for ground confirmation through field measurements.

By and large, one of the significant outcomes of this study is the fact that the so-called “bottom effects” were proved to be of no relevance in the model predictions, despite the shallow depth of the study lake, bearing in mind that previous studies using this approach were essentially limited to larger lakes with greater depth.

Acknowledgements

The European Space Agency ESA is gratefully acknowledged for the provision of MERIS data within the framework of TIGER/TREES project. The authors wish to thank ITC fellows for their support and contribution, and the invaluable assistance of Dr. Suhyb Salama of ITC (University of Twente, The Netherlands) is particularly appreciated.

References

- [1] Dekker, A.G., Vos, R.J. and Peters, S.W.M. (2001) Comparison of Remote Sensing Data, Model Results and *in Situ* Data for Total Suspended Matter (SPM) in the Southern Frisian Lakes. *Science of the Total Environment*, **268**, 197-214. [http://dx.doi.org/10.1016/S0048-9697\(00\)00679-3](http://dx.doi.org/10.1016/S0048-9697(00)00679-3)
- [2] Dall'Olmo, G. and Gitelson, A.A. (2006) Effect of Bio-Optical Parameter Variability and Uncertainties in Reflectance Measurements on the Remote Estimation of Chlorophyll-A Concentration in Turbid Productive Waters: Modeling Results. *Applied Optics*, **45**, 3577-3592. <http://dx.doi.org/10.1364/AO.45.003577>
- [3] IOCCG (2006) Remote Sensing of Inherent Optical Properties: Fundamentals, Tests of Algorithms, and Applications. In: Lee, Z.P., Ed., *Reports of the International Ocean-Colour Coordinating Group*, Dartmouth, Vol. 5. <http://www.ioccg.org/reports/report5.pdf>
- [4] Gohin, F., Loyer, S., Lunven, M., Labry, C., Froidefond, J.-M., Delmas, D., *et al.* (2005) Satellite-Derived Parameters for Biological Modeling of Coastal Waters: Illustration over the Eastern Continental Shelf of the Bay of Biscay. *Remote Sensing of environment*, **95**, 29-46. <http://dx.doi.org/10.1016/j.rse.2004.11.007>
- [5] Schalles, J.F. (2006) Optical Remote Sensing Techniques to Estimate Phytoplankton Chlorophyll A Concentrations in Coastal Waters with Varying Suspended Matter and CDOM Concentrations. In: Richardson, L. and Ledrew, E., Eds., *Remote Sensing of Aquatic Coastal Ecosystem Processes: Science and Management Applications*, Springer, 27-79. http://dx.doi.org/10.1007/1-4020-3968-9_3
- [6] Giardino, C.G., Brando, V.E., Dekker, A.G., Strömbeck, N. and Candiani, G. (2006) Assessment of Water Quality in Lake Garda (Italy) Using Hyperion. *Remote Sensing of Environment*, **109**, 183-195. <http://dx.doi.org/10.1016/j.rse.2006.12.017>
- [7] Schroeder, Th., Schaale, M. and Fischer, J. (2007) Retrieval of Atmospheric and Oceanic Properties from MERIS Measurements: A New Case-2 Water Processor for BEAM. *International Journal of Remote Sensing*, **28**, 5627-5632. <http://dx.doi.org/10.1080/01431160701601774>
- [8] Schroeder, Th. and Fischer, J. (2003) Atmospheric Correction of MERIS Imagery above Case-2 Waters. *Proceedings of the 2003 MERIS User Workshop*, ESA ESRIN, Frascati.
- [9] Doerffer, R. and Schiller, H. (2007) The MERIS Case 2 Water Algorithm. *International Journal of Remote Sensing*, **28**, 517-535. <http://dx.doi.org/10.1080/01431160600821127>
- [10] Doerffer, R. and Fischer, J. (1994) Concentrations of Chlorophyll, Suspended Matter and Gelbstoff in Case II Waters Derived from Satellite CZCS Data with Inverse Modeling Methods. *Journal of Geophysical Research-Oceans*, **99**, 7457-7466. <http://dx.doi.org/10.1029/93JC02523>
- [11] Lindell, T., Pierson, D., Premazzi, G. and Zilioli, E. (1999) Manual for Monitoring European Lakes Using Remote Sensing Techniques EUR Report, Vol. 18665, Office for Official Publications of the European Communities (EN), Luxembourg.
- [12] Härmä, P., Vepsäläinen, J., Hannonen, T., Pyhälähti, T., Kämäri, J., Kallio, K., *et al.* (2001) Detection of Water Quality Using Simulated Satellite Data and Semiempirical Algorithms in Finland. *Science of the Total Environment*, **268**, 107-121. [http://dx.doi.org/10.1016/S0048-9697\(00\)00688-4](http://dx.doi.org/10.1016/S0048-9697(00)00688-4)
- [13] Brando, V.E. and Dekker, A.G. (2003) Satellite Hyperspectral Remote Sensing for Estimating Estuarine and Coastal Water Quality. *IEEE Transactions on Geoscience and Remote Sensing*, **41**, 1378-1387. <http://dx.doi.org/10.1109/TGRS.2003.812907>
- [14] Schroeder, Th. and Schaale, M. (2005) Brief Documentation of the FUB/WeW WATER Processor—A Plug-In for MERIS/(A)ATSR Toolbox (BEAM). <http://www.brockmann-consult.de/beam/plugins.html>
- [15] IOCCG (2000) Remote Sensing of Ocean Colour in Coastal, and Other Optically-Complex, Waters. In: Sathyendranath, S., Ed., *Reports of the International Ocean-Colour Coordinating Group*, No. 3, IOCCG, Dartmouth.
- [16] Sathyendranath, S. and Platt, T. (1997) Analytic Model of Ocean Color. *Applied Optics*, **36**, 2620-2629. <http://dx.doi.org/10.1364/AO.36.002620>
- [17] Gordon, H.R., Brown, O.B., Evans, R.H., Brown, J.W., Smith, R.C., Baker, K.S., *et al.* (1988) A Semianalytic Radiance Model of Ocean Color. *Journal of Geophysical Research*, **93**, 10909-10924. <http://dx.doi.org/10.1029/JD093iD09p10909>
- [18] Walker, R.E. (1994) *Marine Light Field Statistics*. Wiley, New York.
- [19] Arfi, R., Ba, N., Bouvy, M., Corbin, C., Diop, Y., Ka, S., Lebihan, F., Mboup, M., Ndour, E.H., Pagano, M. and Sané, S. (2003) Lac de Guiers (Sénégal). Conditions environnementales et communautés planctoniques. Document Centre IRD Dakar, 77 p.
- [20] Traoré, O. (1995) Etude des échanges hydrogéologiques entre les eaux du lac de Guiers et la nappe alluviale superficielle sous-jacente (Sénégal) Mem. DEA Institut des sciences de l'environnement, 107 p.

- [21] Thiam, A. and Ouattara, M. (1997) Un macrophyte en voie d'invasion du lac de Guiers (Sénégal): *Potamogeton schweinfurthii* A. Bennett (Potamogetonaceae). *Journal de Botanique, Société Botanique de France*, **4**, 71-78.
- [22] Cogels, F.X., Coly, A. and Niang, A. (1997) Impact of Dam Construction on the Hydrological Regime and Quality of a Sahelian Lake in the River Senegal Basin. *Regulated Rivers: Research & Management*, **13**, 27-41.
- [23] Bamba, S.B. (1985) Première approche de la physico-chimie des eaux interstitielles des sédiments du Lac Guiers (Sénégal). Mémoire de DEA, UCAD, Faculté des Sciences, 60 p.
- [24] Sane, S. (2006) Contrôle environnemental de la production primaire du lac de Guiers au Nord du Sénégal. Thèse doct. 3e cycle UCAD, Dakar, 187 p.
- [25] Ba, N. (2006) La communauté phytoplanctonique du lac de Guiers (senegal): Types d'associations fonctionnelles et approches expérimentales des facteurs de régulation. Thèse doct. 3e cycle UCAD, Dakar, 144 p.
- [26] Carl Bro International (1999) Etude bathymétrique et limnologique du lac de Guiers. Rapport de synthèse Hydroconsult international, SGPRE, 119 p.
- [27] Rast, M. (1999) The ESA Medium Resolution Imaging Spectrometer MERIS—A Review of the Instrument and Its Mission. *International Journal of Remote Sensing*, **20**, 1679-1680. <http://dx.doi.org/10.1080/014311699212416>
- [28] Diop, S., Wade, S. and Tijani, M.N. (2008) Analysis of MERIS Data for Lake Guiers' (SENEGAL) Water Quality Assessment-Preliminary Results. *Proceedings of the 2nd MERIS/(A)ATSR User Workshop*, Frascati, 22-26 September 2008, 8 p.
https://earth.esa.int/web/guest/missions/esa-operational-eo-missions/envisat/content/-/asset_publisher/V1xF/content/2nd-meris-a-atrsr-user-workshop-6094
- [29] Fomferra, N. and Brockmann, C. (2005) Beam—The ENVISAT MERIS and AATSR Toolbox. *Proceedings of the MERIS/(A)ATSR User Workshop*, Frascati, 26-30 September 2005.
- [30] Binding, C.E., Jerome, J.H., Bukata, R.P. and Booty, W.G. (2007) Spectral Absorption Properties of Dissolved and Particulate Matter in Lake Erie. *Remote Sensing of Environment*, **112**, 1702-1711.
<http://dx.doi.org/10.1016/j.rse.2007.08.017>
- [31] Brock, T.C.M., Bos, A.R., Crum, S.J.H. and Gylstra, R. (1995) The Model Ecosystem Approach in Ecotoxicology as Illustrated with a Study on the Fate and Effects of an Insecticide in Stagnant Freshwater Microcosms. In: Hock, B. and Niessner, R., Eds., *Immunochemical Detection of Pesticides and Their Metabolites in the Water Cycle (DFG Research Report)*, VCH, Weinheim, Basel, Cambridge, New York and Tokyo, 167-185.
- [32] Thomann, R.V. and Mueller, J.A. (1987) Principles of Surface Water Quality Modeling and Control. Harper-Collins, New York, 644 p.
- [33] Lung, W.S. (1996) Fate and Transport Modeling Using a Numerical Tracer. *Water Resources Research*, **32**, 171-178.
<http://dx.doi.org/10.1029/95WR02918>